

YMTHE, Volume 28

## **Supplemental Information**

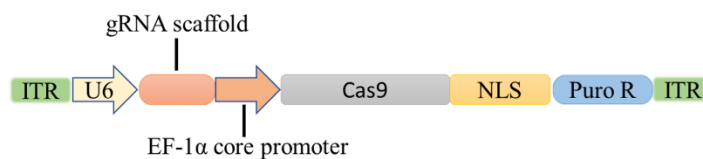
### **CRISPR/Cas9-Mediated miR-29b Editing as a Treatment of Different Types of Muscle Atrophy in Mice**

**Jin Li, Lijun Wang, Xuejiao Hua, Haifei Tang, Rui Chen, Tingting Yang, Saumya Das, and Junjie Xiao**

**Supplemental Figures and Legends:**

**Figure S1**

**a**



**b**

	Forward primer(5'-3')	Reverse primer(5'-3')	Locus
1	GGGACTCGAGCACTCTATGTT	AGGGTCATTAGCAGGGTTCC	chr1:+196863288
2	TCATCGGACCTTGACAGCTC	TGTGCCAGGCCAGAGAAAA	chr9:-101867160
3	AGCCGAGCTATCAATGGGC	TTCATCTGCATTCTGCGCTGT	chr2:-44912669
4	CTGCATTGAGTGCCTTAGCG	GACCATTGGAAACCGTGTGA	chr11:-26661876
5	GCACTGGGGACATAGGTGAG	AGCCACCTTGGCAATAGAC	chr5:-68275574
6	CAGTGAGCTTCACAGTTTGTCT	GAGTCATACAGTATTTAGGCTGCT	chrX:+93743993
7	AAGGCTGAATGCCGTTCACT	GGCAAGAAGAACCTGGGACA	chr16:+15872481
8	ATGCAGCAGATGCCAGACTT	CTCATGAGCACAGGAGCCAA	chr15:-66654630
9	GACCACCACAATCGGCTGTA	GTTCTTGGCTCCCCTGACTC	chr11:-98951837
10	TGGCTGCCAATACCTATGCT	AGCCATCCCCTCGACTCAAA	chr4:+40629962

**c**

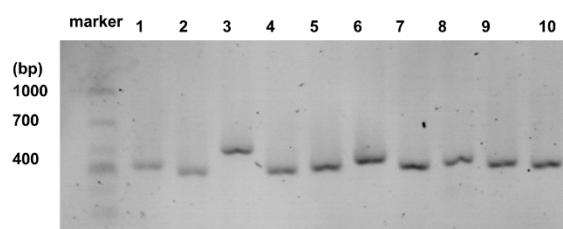


**Figure S1. Backbone of lentiCRISPRv2 and T7E1 analysis for the top genome-wide off-target sites with genomic DNA from C2C12 myotubes. (a)** The backbone of lentiCRISPRv2 (Addgene plasmid # 52961). **(b)** The predicted top 10 potential off-target sites in the mouse genomic (<http://crispr.mit.edu/>). **(c)** No significant off-target mutagenesis was detected in T7E1 cleavage assay.

**Figure S2**

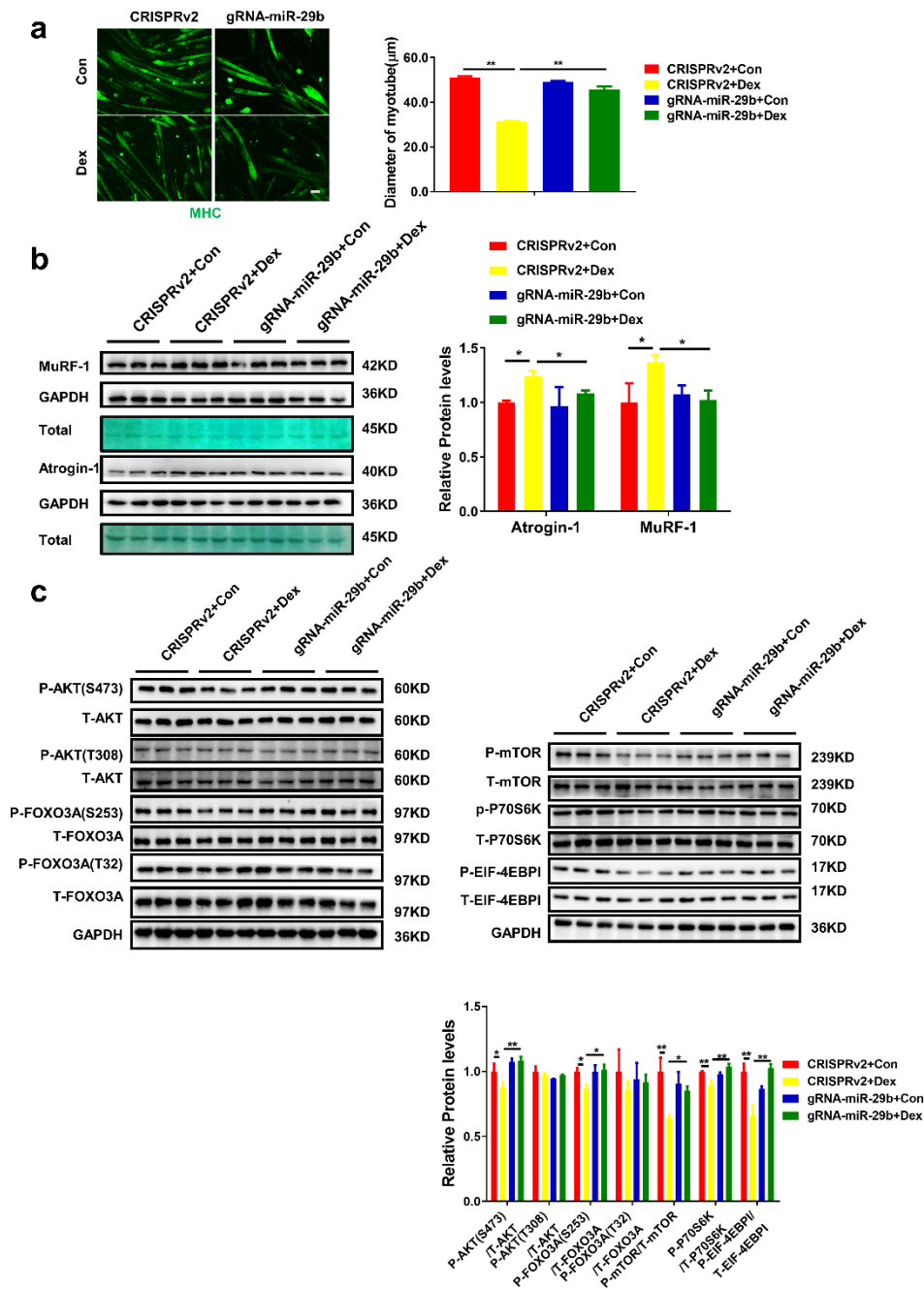
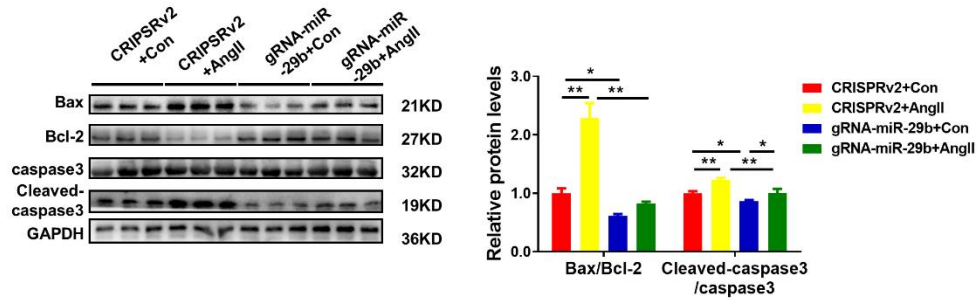


**Figure S2. CRISPR/Cas9 mediated miR-29b editing prevents dexamethasone-induced atrophy in cultured C2C12 myotubes.** (a) Immunofluorescence staining for diameters of C2C12 myotubes in dexamethasone (Dex)-induced atrophy with or without SpCRISPR-gRNA-miR-29b treatment (n=3, scale bar: 100 µm). (b) Western blot and quantitative analysis of MuRF-1 and Atrogin-1 protein levels in dexamethasone-induced atrophy with or without SpCRISPR-gRNA-miR-29b treatment (n=3). GAPDH protein and total proteins are stained for control. (c) Western blot and quantitative analysis for the AKT/FOXO3A/mTOR pathway (AKT, FOXO3A, mTOR, P70S6K, EIF-4EBP1) in C2C12 myotubes (n=3). One-way ANOVA test was performed to compare multiple groups followed by Bonferroni or Dunnett T3's post hoc test based on homogeneity of variance test. \*p<0.05, \*\*p<0.01 versus respective control.

## Figure S3

**a**



**b**

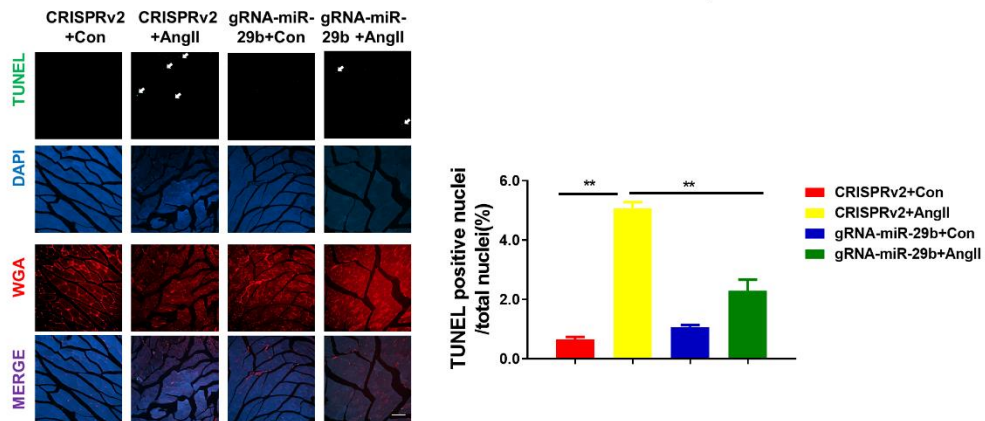


**Figure S3. CRISPR/Cas9 mediated miR-29b editing prevents AngII-induced apoptosis. (a)** Western blot and quantitative analysis of Bcl-2, Bax, Cleaved-caspase 3, caspase 3 protein levels in AngII-treated mice with or without SpCRISPR-gRNA-miR-29b treatment (n=3). **(b)** TUNEL staining of Gastrocnemius muscle in AngII-treated mice with or without SpCRISPR-gRNA-miR-29b treatment (n=4, scale bar: 20 μm). AngII, Angiotensin II. One-way ANOVA test was performed to compare multiple groups followed by Bonferroni or Dunnett T3's post hoc test based on homogeneity of variance test. \*p<0.05, \*\*p<0.01 versus respective control. Data are represented as mean±s.e.m.

**Figure S4**

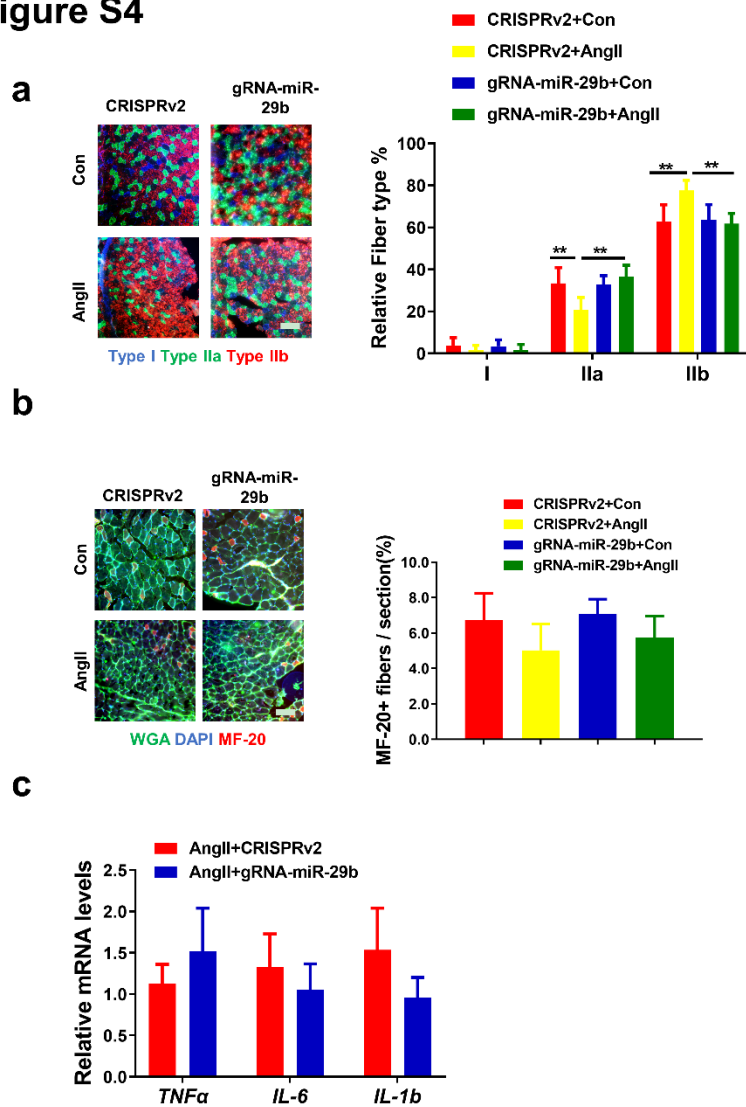


**Figure S4. The effects of CRISPR/Cas9 treatment on muscle fiber composition, regeneration, and inflammation in AngII-induced muscle atrophy. (a)** Immunofluorescence staining of myosin heavy chains isotypes (MHC) in Gastrocnemius muscle from indicated groups (n=6, scale bar: 100  $\mu$ m). **(b)** Immunostaining for MF-20 from Gastrocnemius muscle in AngII-treated mice with or without SpCRISPR-gRNA-miR-29b treatment (n=4, scale bar: 100  $\mu$ m). **(c)** RT-PCR analysis the mRNA expression levels of the inflammation factors (*TNF $\alpha$* , *IL-6*, and *IL-1b*) in AngII-treated mice with or without SpCRISPR-gRNA-miR-29b treatment (n=6). AngII, Angiotensin II. One-way ANOVA test was performed to compare multiple groups followed by Bonferroni or Dunnett T3's post hoc test based on homogeneity of variance test (a-b). An unpaired, two-tailed Student's t-test was used for comparisons between two groups (c). \*\*p<0.01 versus respective control. Data are represented as mean $\pm$ s.e.m.

**Figure S5**

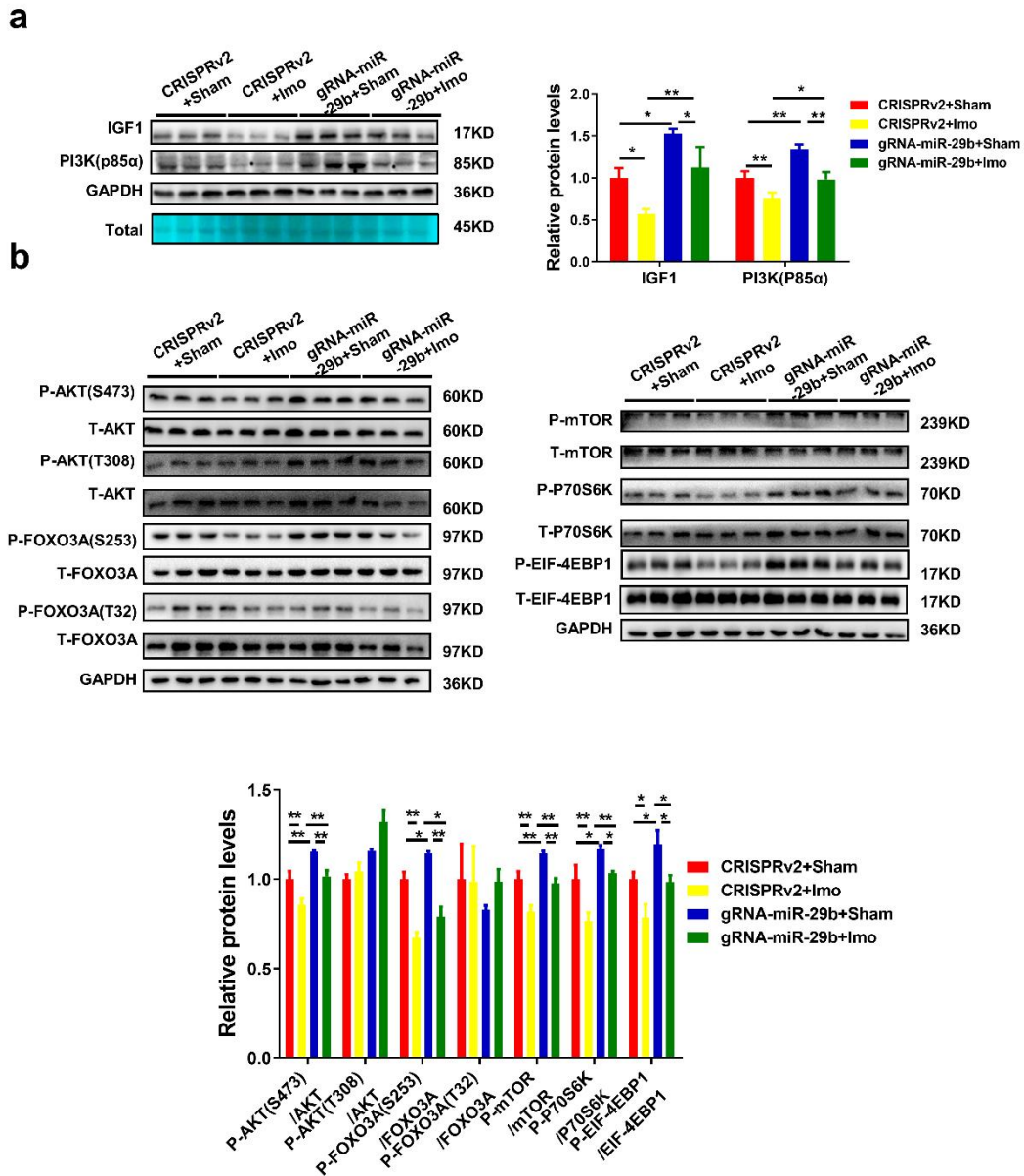


**Figure S5. CRISPR/Cas9 mediated miR-29b editing prevents immobilization-induced atrophy effects through activation of the AKT-FOXO3A-mTOR signaling pathway. (a)** Western blot and quantitative analysis of extracts from Gastrocnemius muscle to detect IGF1 and PI3K(p85 $\alpha$ ) protein in SpCRISPR-gRNA-miR-29b administration mice compared to control (n=3). GAPDH protein and total proteins are stained for control. **(b)** Western blot and quantitative analysis of the AKT/FOXO3A/mTOR pathway (AKT, FOXO3A, mTOR, P70S6K, EIF-4EBP1) in immobilization-treated mice with or without SpCRISPR-gRNA-miR-29b treatment (n=3). Imo, immobilization. One-way ANOVA test was performed to compare multiple groups followed by Bonferroni or Dunnett T3's post hoc test based on homogeneity of variance test. \*p<0.05, \*\*p<0.01 versus respective control. Data are represented as mean $\pm$ s.e.m.

## Figure S6

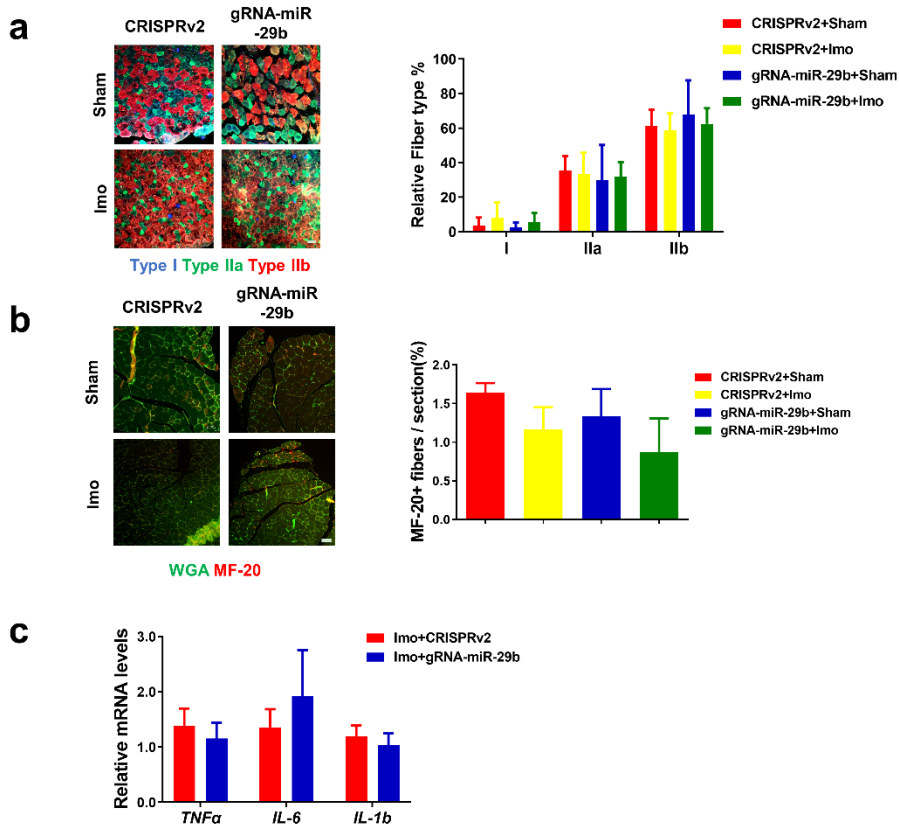


**Figure S6. The effects of CRISPR/Cas9 treatment on muscle fiber composition, regeneration, and inflammation in immobilization-induced muscle atrophy.** (a) The fiber type composition (n=5, scale bar: 100  $\mu$ m), and (b) muscle regeneration (n=3,5,3,5, scale bar: 100  $\mu$ m) in immobilization-induced muscle atrophy were presented by immunofluorescence staining. (c) RT-PCR analysis the mRNA expression levels of the inflammation factors (*TNF $\alpha$* , *IL-6*, and *IL-1b*) in immobilization-treated mice with or without SpCRISPR-gRNA-miR-29b treatment (n=6). Imo, immobilization. One-way ANOVA test was performed to compare multiple groups followed by Bonferroni or Dunnett T3's post hoc test based on homogeneity of variance test (a-b). An unpaired, two-tailed Student's t-test was used for comparisons between two groups (c). Data are represented as mean $\pm$ s.e.m.

**Figure S7**

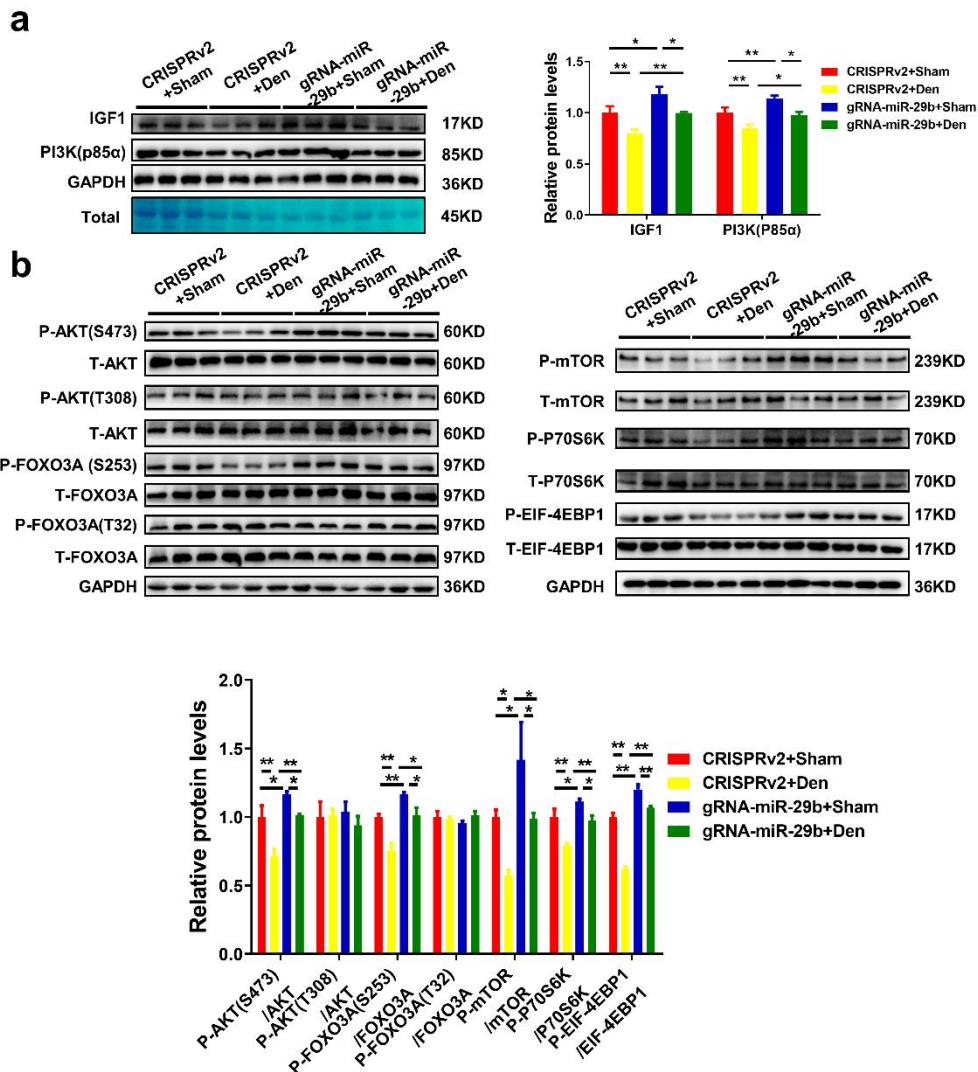


**Figure S7. CRISPR/Cas9 mediated miR-29b editing prevents denervation-induced atrophy effects through activation of the AKT-FOXO3A-mTOR signaling pathway.** (a) Western blot and quantitative analysis of extracts from Gastrocnemius muscle to detect IGF1 and PI3K(p85α) protein is shown in SpCRISPR-gRNA-miR-29b administration mice compared to control (n=3). GAPDH protein and total proteins are stained for control. (b) Western blot and quantitative analysis of the AKT/FOXO3A/mTOR pathway (AKT, FOXO3A, mTOR, P70S6K, EIF-4EBP1) in denervation-treated mice with or without SpCRISPR-gRNA-miR-29b treatment (n=3). Den, denervation. One-way ANOVA test was performed to compare multiple groups followed by Bonferroni or Dunnett T3's post hoc test based on homogeneity of variance test. \*p<0.05, \*\*p<0.01 versus respective control. Data are represented as mean±s.e.m.



## Figure S8

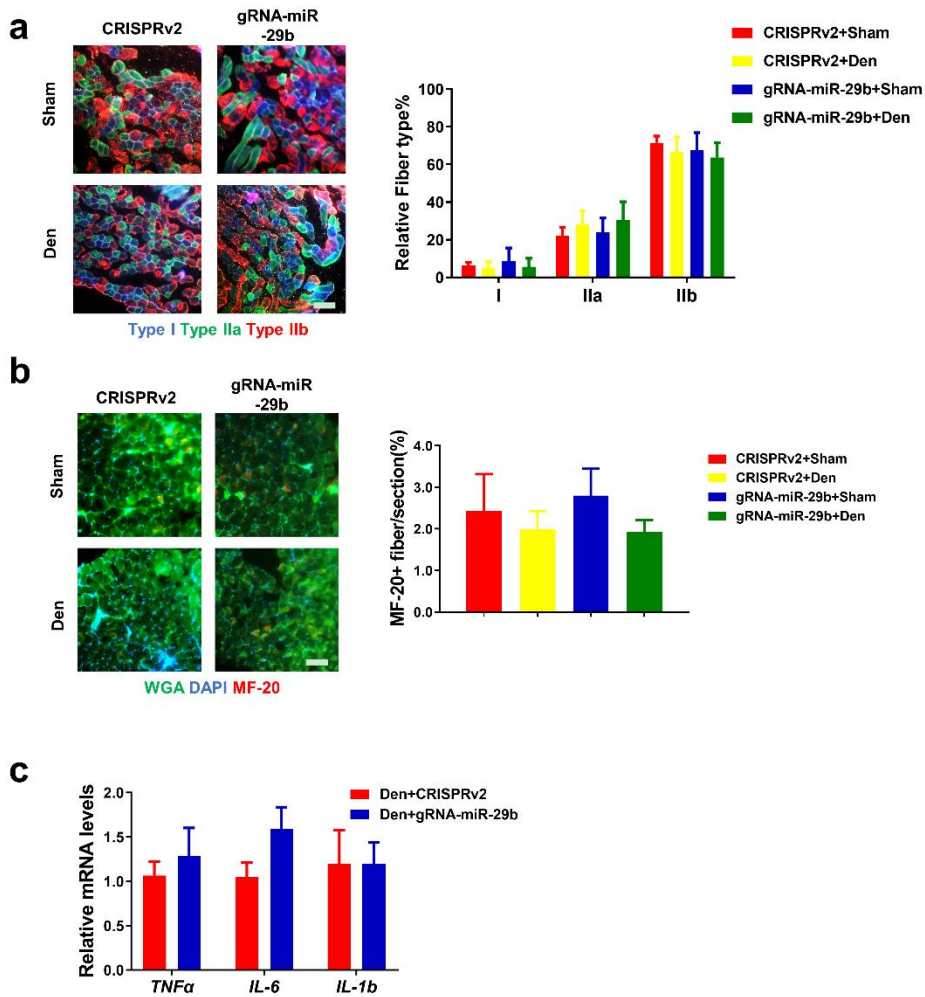


**Figure S8. CRISPR/Cas9 treatment did not affect muscle fiber composition, regeneration, and inflammation in denervation-induced muscle atrophy.** (a) The fiber type composition (n=6, scale bar: 100  $\mu$ m), (b) muscle regeneration (n=4, scale bar: 100  $\mu$ m), and (c) inflammation (n=6) in denervation-induced muscle atrophy were shown as indicated groups. Den, denervation. One-way ANOVA test was performed to compare multiple groups followed by Bonferroni or Dunnett T3's post hoc test based on homogeneity of variance test (a-b). An unpaired, two-tailed Student's t-test was used for comparisons between two groups (c). Data are represented as mean $\pm$ s.e.m.

## Figure S9

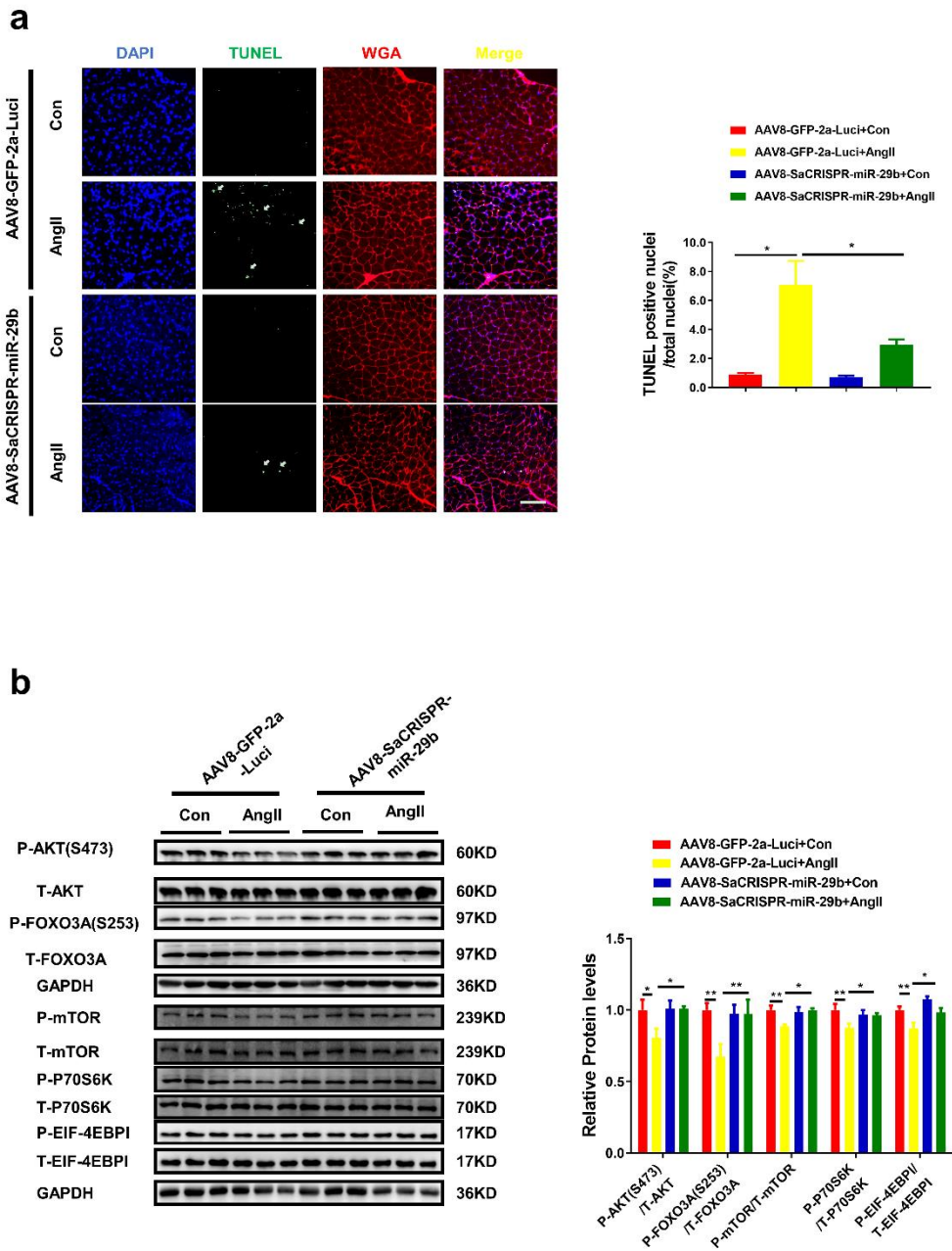


**Figure S9. AAV8-CRISPR/SaCas9 mediated miR-29b editing prevents AngII-induced apoptosis and activates of AKT-FOXO3A-mTOR signaling pathway.** (a) TUNEL staining of Gastrocnemius muscle in AngII-treated mice with or without AAV8-SaCRISPR-miR-29b treatment (n=4, scale bar: 100  $\mu$ m). (b) Western blot and quantitative analysis of the relative phosphorylation levels of AKT(S473), FOXO3A(S253), mTOR, P70S6K and EIF-4EBP1 in AngII-induced muscle atrophy with or without AAV8-SaCRISPR-miR-29b-treated treatment (n=3). AngII, Angiotensin II. One-way ANOVA test was performed to compare multiple groups followed by Bonferroni or Dunnett T3's post hoc test based on homogeneity of variance test. \*p<0.05, \*\*p<0.01 versus respective control. Data are represented as mean $\pm$ s.e.m.

## Figure S10

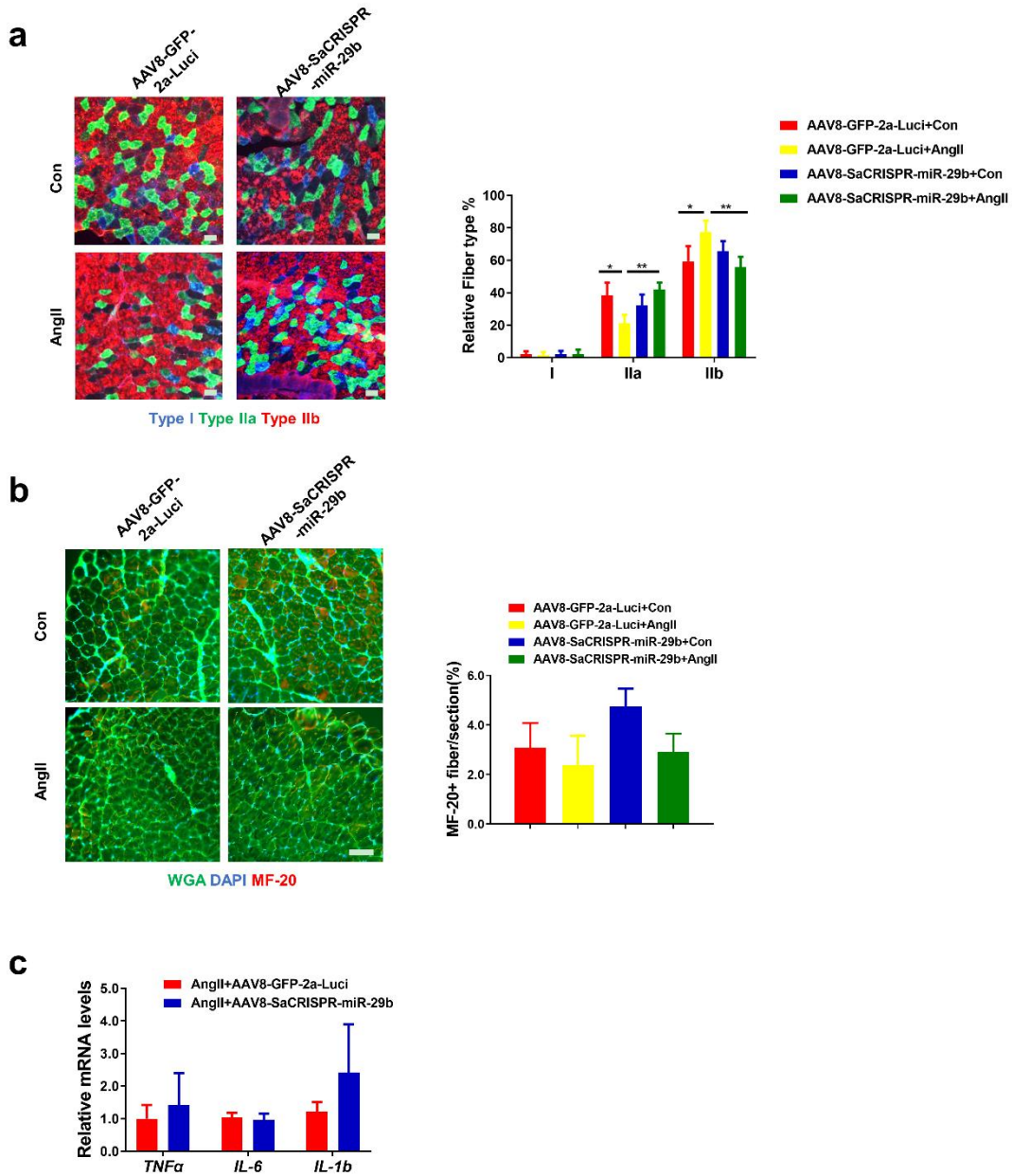


**Figure S10. The effects of AAV8-CRISPR/SaCas9 treatment on muscle fiber composition, regeneration, and inflammation in AngII-induced muscle atrophy.** (a) Immunofluorescence staining of myosin heavy chains isotypes (MHC) in AngII-induced atrophy are presented (n=4, scale bar: 100  $\mu$ m). (b) Immunostaining for MF-20 is shown as indicated groups (n=4, scale bar: 100  $\mu$ m). (c) RT-PCR analysis the expression of inflammation factors (*TNF $\alpha$* , *IL-6*, and *IL-1 $\beta$* ) in AngII-induced muscle atrophy as indicated groups (n=8,7). AngII, Angiotensin II. One-way ANOVA test was performed to compare multiple groups followed by Bonferroni or Dunnett T3's post hoc test based on homogeneity of variance test (a-b). An unpaired, two-tailed Student's t-test was used for comparisons between two groups (c). \*p<0.05, \*\*p<0.01 versus respective control. Data are represented as mean $\pm$ s.e.m.

## Figure S11

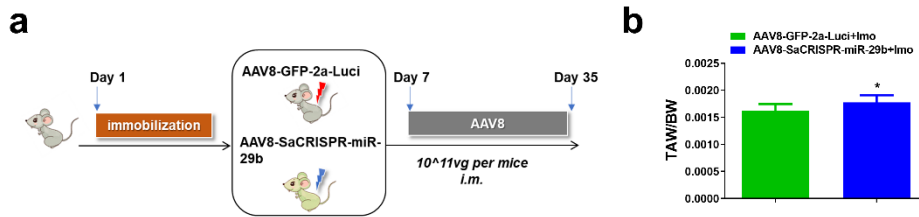


**Figure S11. AAV8-CRISPR/SaCas9 mediated miR-29b editing prevents immobilization induced-muscle atrophy in vivo.** (a) The schedule of immobilization (Imo)-induced atrophy mice model and virus injection establishment. (b) Tibialis anterior weight/body weight ratio (TAW/BW) ratio are shown in Imo-treated mice with or without AAV8-SaCRISPR-miR-29b injection treatment (n=6,7). An unpaired, two-tailed Student's t-test was used for comparisons between two groups (b). \*p<0.05 versus respective control. Data are represented as mean±s.e.m.

## Figure S12

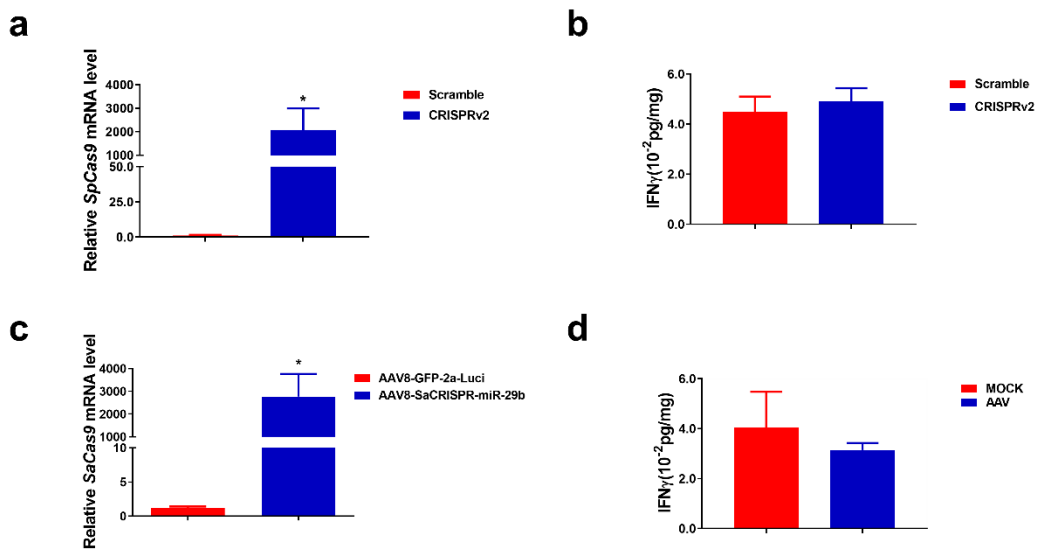


**Figure S12. Expression of both the SpCas9 and SaCas9 mRNA and the production of IFN $\gamma$  in the endpoints of the experiments.** (a) RT-PCR analysis of *SpCas9* mRNA expression level after 2 weeks for lentivirus-delivered CRISPR/spCas9 (n=6). (b) The production of IFN $\gamma$  was evaluated by enzyme-linked immunosorbent assay (ELISA) after 2 weeks for lentivirus-delivered CRISPR/spCas9 (n=5). (c) RT-PCR analysis of *SaCas9* mRNA expression level after 4 weeks for AAV8-delivered /SaCas9 (n=14). (d) The production of IFN $\gamma$  was evaluated by ELISA after 4 weeks for AAV8-delivered /SaCas9 (n=3,6). An unpaired, two-tailed Student's t-test was used for comparisons between two groups. \*p<0.05 versus respective control. Data are represented as mean±s.e.m.

**Supplemental Tables:**

**Table S1. gRNAs sequences used in this study.**

---

	<b>Sequence</b>	<b>PAM</b>
A	AGGAAGCTGGTTTCATATGG	TGG
B	TTCAGGAAGCTGGTTTCATA	TGG
C	CCATTTGAAATCAGTGTTTT	AGG
D	CCTAAAACACTGATTCAAA	TGG

---

**Table S2. qPCR primers used in this study.**

<b>Gene</b>	<b>Forward (5'-3')</b>	<b>Reverse (5'-3')</b>
<i>mmu-IL-6</i>	TAGTCCTTCCTACCCCAATTTCC	TTGGTCCTTAGCCACTCCTTC
<i>mmu-TNF<math>\alpha</math></i>	AGGCACTCCCCCAAAGATG	CCACTTGGTGGTTTGTGAGTG
<i>mmu-IL-1b</i>	GCAACTGTTCTGAACTCAACT	ATCTTTTGGGGTCCGTCAACT
<i>SaCas9</i>	GGCGTCAGACTGTTCAAGGA	GGTCGGTCAGCAGGTTGTAA
<i>SpCas9</i>	CATCGAGCAGATCAGCGAGT	CGATCCGTGTCTCGTACAGG
<i>mmu-18s</i>	TCAAGAACGAAAGTCGGAGG	GGACATCTAAGGGCATCAC

## **Supplemental Methods:**

### **Cultured C2C12 myotubes staining**

To determine the diameter of myotubes in vitro, C2C12 myotubes were fixed with 4% paraformaldehyde, permeabilized with 0.5% Triton X-100, and blocked with 5% BSA. Then the primary antibody anti-MHC (MF-20, 1:100, DSHB) was used to specific label myotubes, FITC-AffiniPure Rabbit Anti-Mouse IgG (H+L) (1:500, Jackson) was used as secondary antibody. DAPI was subjected to nuclear staining. Images were captured by fluorescence microscope (Leica, Wetzlar, Germany) and the diameter of myotubes was measured by Image J.

### **Skeletal Muscle Histology and Immunofluorescence**

For skeletal muscle fiber types analyses, skeletal muscle was obtained and embedded in OCT, and snap frozen in cold liquid nitrogen. Samples were cut at 10  $\mu\text{m}$  per section. The section was incubated in room temperature (RT) for 20min, fixed with 4% paraformaldehyde in RT for another 20min. Then, sections were blocked with 5% BSA in PBS, incubated with anti-MyHC-I (BA-D5, 1:3, DSHB), anti-MyHC-IIA (SC-71, 1:10, DSHB), anti-MyHC-IIb (BF-F3, 1:3, DSHB) overnight at 4°C. After washed with PBS, the secondary antibodies were applied at a dilution of 1:100, the Alexa 350 anti-mouse IgG2b (Invitrogen, USA), Alexa 488 anti-mouse IgG1 (Invitrogen, USA), and Alexa 555 anti-mouse IgM (Invitrogen, USA) were used. Then the images were captured by fluorescence microscope (Zeiss, Oberkochen Germany).

For regeneration analysis, frozen sections of 10 $\mu\text{m}$  were used after rewarming, permeability and blocking, the sections were incubated with MF-20 (1:50, DSHB) overnight at 4°C. Then WGA conjugates (Invitrogen, USA) was incubated to show the outline of muscle fibers. Secondary antibody Cy3-AffiniPure Rabbit Anti-Mouse IgG (H+L) (1:500, Jackson, USA) was incubated at RT for 1 h to label MF-20, and 4,6-Diamidin-2-phenylindol (DAPI, Sigma, USA) was stained for nuclei. The images were captured using fluorescence microscope (Zeiss, Oberkochen Germany).